

556841
P20

NASA Technical Memorandum 102609

**CONICAL EULER SOLUTION FOR A HIGHLY-SWEPT DELTA WING
UNDERGOING WING-ROCK MOTION**

**ELIZABETH M. LEE
JOHN T. BATINA**

MARCH 1990

**(NASA-TM-102609) CONICAL EULER SOLUTION FOR
A HIGHLY-SWEPT DELTA WING UNDERGOING
WING-ROCK MOTION (NASA) 18 p CSCL 01A**

N90-19211

Unclass

G3/02 0272294



**National Aeronautics and
Space Administration**

**Langley Research Center
Hampton, Virginia 23665-5225**

CONICAL EULER SOLUTION FOR A HIGHLY-SWEPT DELTA WING UNDERGOING WING-ROCK MOTION

Elizabeth M. Lee
John T. Batina
NASA Langley Research Center
Hampton, Virginia 23665-5225

Summary

Modifications to an unsteady conical Euler code for the free-to-roll analysis of highly-swept delta wings are described. The modifications involve the addition of the rolling rigid-body equation of motion for its simultaneous time-integration with the governing flow equations. The flow solver utilized in the Euler code includes a multistage Runge-Kutta time-stepping scheme which uses a finite-volume spatial discretization on an unstructured mesh made up of triangles. Steady and unsteady results are presented for a 75° swept delta wing at a freestream Mach number of 1.2 and an angle of attack of 30°. The unsteady results consist of forced harmonic and free-to-roll calculations. The free-to-roll case exhibits a wing rock response produced by unsteady aerodynamics consistent with the aerodynamics of the forced harmonic results. Similarities are shown with a wing-rock time history from a low-speed wind tunnel test.

Introduction

In recent years, the understanding and prediction of the complex flows about modern aircraft at high angles of attack have been research topics that have generated much interest within the fluid dynamics community.^{1,2} These aircraft typically have thin highly-swept lifting surfaces such as delta wings which produce a vortical flow over the leeward-side of the vehicle at high angles of attack. This vortical flow can have beneficial effects on performance, such as lift augmentation at high- α , but may also have adverse effects such as structural fatigue due to tail buffet and also stability and control problems such as wing rock, wing drop, nose slice, and pitch-up.³ Considerable research has been conducted into the wing-rock phenomenon which is a self-induced, limit-cycle rolling oscillation with, in some cases, a coupled yaw oscillation. Both

experimental and computational methods have been used in these efforts to better understand the basic flow physics involved in this type of unsteady, vortical flow. Experimental investigations into wing rock have been reported by Nguyen et al.⁴ for forced harmonic and free-to-roll motions of an 80° swept delta wing in low speed flow. In Ref. 4, the model was found to undergo wing rock for angles of attack greater than 25°. Levin and Katz⁵ tested both 76° and 80° swept delta wings and found that only the 80° model would exhibit wing rock at high- α . Further studies have been performed by Nelson^{6,7} and co-workers at Notre Dame University. These studies have shown, for example, the time histories of the vortex core position during a cycle of wing rock⁶ and the static and dynamic effects due to vortex breakdown.⁷ Also Ng et al.⁸ have recently reported experimental results obtained in a water tunnel which show wing rock for several different delta wing planforms along with detailed flow visualization diagrams. These studies⁴⁻⁸ have contributed significantly to the understanding of wing rock although much work remains to be done.

Computational methods have also been applied to the prediction of wing rock. Hsu and Lan⁹ presented a nonlinear mathematical model for calculating wing-rock characteristics based on aerodynamic derivatives evaluated using steady-flow aerodynamics at average dynamic conditions. Researchers at Virginia Polytechnic Institute and State University¹⁰⁻¹² have simulated wing rock using an unsteady vortex-lattice method to predict the aerodynamic loads and have integrated the equation of rolling motion using a predictor-corrector method. The methods of both Ref. 9 and Refs. 10-12 predicted with reasonable accuracy the low-speed wing-rock characteristics of the delta wings studied in Refs. 4 and 5. Use of the more modern computational fluid dynamics techniques for the prediction of vortex-dominated flows¹³ has primarily focused on steady applications,¹⁴⁻²¹ although there are notable exceptions where applications have been made to rolling delta wings undergoing forced harmonic motion.²²⁻²⁴ These unsteady methods, although applicable to general time-

dependent vortical flow phenomena, have yet to be applied to problems such as wing rock. The objective of the current research is to study unsteady vortex-dominated flowfields by using the conical Euler equations as an efficient first step to investigating the full three-dimensional problem. The purpose of this paper is to report the recent calculation of a conical Euler solution for a delta wing undergoing wing-rock motion. The flow solver used for this calculation is that of Ref. 24, which involves a Runge-Kutta time-stepping scheme and a finite-volume spatial discretization suited for an unstructured grid. The code was modified to allow for the additional analysis of the free-to-roll case by the inclusion of the rigid-body equation of motion for simultaneous time-integration with the governing flow equations. Results are presented for a highly-swept delta wing which demonstrate the computational simulation of wing rock similar to the experimental investigation of Ref. 7. Of course, the conical Euler assumption is limited to supersonic freestream applications, whereas the test of Ref. 7 was for low-speed flow. The paper presents a brief description of the conical Euler flow solver and free-to-roll analysis, along with results which demonstrate the capability.

Symbols

a_{∞}	freestream speed of sound
C_l	rolling moment coefficient
c	root chord of wing
I_{xx}	mass moment of inertia about longitudinal axis
k	reduced frequency based on one half of the root chord
ℓ	rolling moment
M_{∞}	freestream Mach number
q_{∞}	freestream dynamic pressure
S	planform area
α	angle of attack

$\Delta \bar{t}$	nondimensional global time step
μ_x	structural damping
ρ_∞	freestream density
ϕ	instantaneous roll angle
ϕ_0	harmonic roll angle amplitude

Euler Solution Algorithm

The unsteady conical Euler equations are solved using the multi-stage Runge-Kutta time-stepping scheme of Ref. 24. This algorithm uses a finite-volume spatial discretization for solution on an unstructured grid made up of triangles. The original algorithm of Ref. 24 was a node-based scheme whereby the flow variables are stored at the vertices of the triangles. A second algorithm, a cell-centered scheme, was employed in the present study. This second scheme is based on unpublished work of the second author. In the cell-centered scheme, the flow variables are stored at the centroids of the triangles. In both algorithms, artificial dissipation is added explicitly to prevent oscillations near shock waves and to damp high-frequency uncoupled error modes. Specifically, an adaptive blend of harmonic and biharmonic operators is used, corresponding to second and fourth difference dissipation, respectively. The biharmonic operator provides a background dissipation to damp high frequency errors and the harmonic operator prevents oscillations near shock waves. The algorithms also employ enthalpy damping, local time stepping, and implicit residual smoothing to accelerate convergence to steady state. The local time stepping uses the maximum allowable step size at each grid point for the node-based scheme and for each triangle in the cell-centered scheme, as determined by a local stability analysis. The implicit residual smoothing permits the use of local time steps that are larger than those imposed by the Courant-Fredricks-Lewy stability condition. This is achieved by averaging the

residuals implicitly with neighboring values. A time-accurate version of the residual smoothing is also used for global time-stepping during unsteady applications of the code.

With respect to boundary conditions, freestream conditions are applied along the farfield boundary, and a reasonably large computational grid is used so that the bow shock is captured as a part of the solution. A flow tangency (or slip) condition is applied to the inner boundary which represents the wing. Also, for unsteady calculations, the grid is moved as a rigid body to conform to the instantaneous position of the wing. In this application, grid speeds are computed at the nodes and are included in the governing equations to account for the relative motion between the grid and the fluid.

Free-to-Roll Analysis

In this section, the roll equation of motion and the time-marching solution procedure are described.

Roll Equation of Motion

The equation of motion for a rolling delta wing can be expressed as

$$I_{xx} \ddot{\phi} = \ell - \mu_x \dot{\phi} \quad (1)$$

where ϕ is the roll angle which is positive clockwise when viewed from aft, I_{xx} is the mass moment of inertia about the longitudinal axis, ℓ is the aerodynamic rolling moment also positive clockwise, and μ_x is a structural damping term (dot superscripts indicate differentiation with respect to time). In order to nondimensionalize Eq. (1), the angular rates are multiplied by the root chord of the delta wing, c , and divided by the freestream speed of sound, a_∞ . The rolling moment coefficient is defined as

$$C_l = \frac{\ell}{q_\infty S c} \quad (2)$$

where q_∞ is the freestream dynamic pressure and S is the planform area. The nondimensional rolling equation of motion can then be written as

$$\phi'' = C_1 C_\ell - C_2 \phi' \quad (3)$$

where

$$C_1 = \frac{M_\infty^2 S c^3 \rho_\infty}{2 I_{xx}} \quad (4a)$$

$$C_2 = \frac{\mu_x c}{a_\infty I_{xx}} \quad (4b)$$

Note that the prime superscripts indicate differentiation with respect to nondimensional time. The structural damping term is added to simulate a sting bearing mount. This type of bearing mount was used in the low-speed wind tunnel investigations of wing rock reported in Refs. 4-7.

Time-Marching Solution

The solution procedure for the time integration of Eq. (3) is based on a finite difference representation of the time derivatives. The time derivatives are expressed in terms of second-order-accurate finite-difference approximations. After substituting these expressions into Eq. (3), the roll angle at time level $n+1$ can be expressed in terms of the roll angle at previous time levels as

$$\begin{aligned} \phi^{n+1} = & [C_1 C_\ell^{n+1} \Delta \bar{t}^2 + (5 + 2 C_2 \Delta \bar{t}) \phi^n \\ & - (4 + \frac{1}{2} C_2 \Delta \bar{t}) \phi^{n-1} + \phi^{n-2}] / [\frac{3}{2} C_2 \Delta \bar{t} + 2] \end{aligned} \quad (5)$$

The rolling moment at time level $n+1$, C_ℓ^{n+1} , is estimated from a linear extrapolation of C_ℓ at the previous two time levels. This predicted value of C_ℓ is used to determine the roll angle at time level $n+1$, ϕ^{n+1} . The flowfield is then calculated about the wing at this roll angle, and the actual value of the rolling moment coefficient is determined. The

rolling moment coefficient is then updated for use in the next time step. Due to the explicit time-marching of the Euler code used in this study, the time steps required for stability were small, and thus, it was not necessary to iterate between the roll angle calculation and the flowfield calculation at each time step. Previous studies of time-marching aeroelastic analyses using a similar explicit scheme have shown this to be the case (R. D. Rausch: Personal Communication, October 31, 1989). For a free-to-roll calculation, steady-state initial conditions are specified for ϕ^{-1} , ϕ^0 , C_l^{-1} , and C_l^0 . An initial angular velocity is imposed to provide an initial perturbation to the wing.

Results and Discussion

Calculations were performed for a 75° delta wing at a freestream Mach number of 1.2 and an angle of attack of 30°. The wing has thickness and sharp leading edges as indicated in the partial view of the grid shown in Fig. 1. The thickness-to-span ratio at this cross section is .025 and the bevel angle is 10°. The grid, which was generated using an advancing front method,²⁵ has a total of 4226 nodes and 8299 elements. The grid was designed to be fine on the leeward side of the wing where the dominant flow features are expected to occur and to be coarse on the windward side of the wing where the flow gradients are expected to be small. All results presented were calculated using the cell-centered scheme.

Steady-state results were obtained to determine the basic character of the vortical flow. The total pressure loss contour lines from this calculation are shown in Fig. 2. These contours indicate that the flow separates from each of the leading edges of the wing producing two large, circular vortices. Note that as the flow accelerates beneath the vortices, vertically oriented shock waves are formed on the outboard portions of the wing. Weaker shock waves are also formed on the top of each vortex. These vertically oriented shocks are located above the core of the vortex. The crossflow velocity vectors for this case, shown in Fig. 3, also indicate the presence of a weak horizontal shock wave

between the vortices. Furthermore, the small lack of symmetry in the results of Figs. 2 and 3 are due to the fact that the grid is not symmetric.

The wing was then forced to oscillate harmonically in roll at a reduced frequency of $k = 0.3$ (based on one half of the root chord) using 4000 steps per cycle of motion. Several values of reduced frequency were investigated, and these results are representative of the lower frequency responses. Three amplitudes of motion were considered including $\phi_o = 5^\circ$, 15° , and 35° . The plots of rolling moment coefficient versus roll angle for each of these cases are shown in Fig. 4. For the smaller amplitude of 5° , the results show a clockwise-oriented loop which would produce a divergent (unstable) response if the wing were free to roll. Similar results are seen for the 15° case although some nonlinear effects are indicated by the "pinching" of the curve at the extreme values of roll angle. At $\phi_o = 35^\circ$, counter-clockwise-oriented loops have formed at the extreme roll angles which, consequently, would have a stabilizing effect on the free-to-roll response.

To demonstrate the free response capability, results were obtained for the structural parameter values and flow conditions listed in Table 1. The initial angular velocity imposed on the wing was $\phi' = 0.003$. The resulting roll angle response is shown in Fig. 5. This response indicates that initially the oscillatory response diverges for small values of roll angle which is consistent with the small amplitude harmonic results of Fig. 4. As the angle increases to around 35° , the rate of divergence decreases due to the stabilizing aerodynamics shown in Fig. 4 for $\phi_o = 35^\circ$, and finally, the response reaches a maximum amplitude of motion at $\phi = 38^\circ$ corresponding to a limit cycle. The reduced frequency of the limit cycle is $k = 0.103$. These results are similar in nature to those obtained by Arena and Nelson⁷ in a low-speed experimental investigation of wing rock. The wing-rock time history from Ref. 7, shown in Fig. 6, was obtained for an 80° swept delta wing at 30° angle of attack. Although the case considered in the present study is

different from that of Ref. 7 (the data from Refs. 4-8 are all for low speed flows whereas the conical Euler code is limited to supersonic freestream applications), the similarity between the two sets of results in Figs. 5 and 6 is noteworthy and gives credibility to the present calculations.

Concluding Remarks

Modifications to an unsteady conical Euler code for the free-to-roll analysis of highly-swept delta wings were described. The modifications involved the addition of the rolling rigid-body equation of motion for its simultaneous time integration with the governing flow equations. The flow solver utilized in the Euler code included a multistage Runge-Kutta time-stepping scheme which used a finite-volume spatial discretization on an unstructured mesh made up of triangles. Steady and unsteady results were presented for a 75° swept delta wing at a freestream Mach number of 1.2 and an angle of attack of 30°. The unsteady results consisted of forced harmonic and free-to-roll calculations. The free-to-roll case exhibited a wing-rock response produced by unsteady aerodynamics consistent with the aerodynamics of the forced harmonic results. Similarities were shown with a wing-rock time history from a low-speed wind tunnel test.

Acknowledgement

The authors would like to acknowledge Ken Morgan and Jaime Peraire of the Imperial College of Science and Technology, London, England, for providing the advancing front method grid generation program that was used to generate the grid in the present study.

References

- ¹High Angle of Attack Aerodynamics, AGARD-LS-121, December 1982; Lecture Series presented March 10-11, 1982 at NASA Langley Research Center, USA, March 15-19, 1982 at von Karman Institute, Rhode-Saint-Genese, Belgium, and March 22-23, 1982 at DFVLR, Gottingen, Germany.
- ²Vortex Flow Aerodynamics, NASA CP-2416, July 1986; Proceedings of a conference sponsored by the NASA Langley Research Center, Hampton, Virginia, and the Air Force Wright Aeronautical Laboratories, Flight Dynamics Laboratory, Wright-Patterson Air Force Base, Ohio; held at NASA Langley Research Center, October 8-10, 1985.
- ³Hamilton, W. T.: Manoeuvre Limitations of Combat Aircraft, AGARD-AR-155A, August 1979.
- ⁴Nguyen, L. T.; Yip, L.; and Chambers, J. R.: Self-Induced Wing Rock of Slender Delta Wings, AIAA Paper No. 81-1883, August 1981.
- ⁵Levin, D.; and Katz, J.: Dynamic Load Measurements with Delta Wings Undergoing Self-Induced Roll Oscillations, Journal of Aircraft, Vol. 21, January 1984, pp. 30-36.
- ⁶Jun, Y. W.; and Nelson, R. C.: Leading-Edge Vortex Dynamics on a Slender Oscillating Wing, Journal of Aircraft, Vol. 25, September 1988, pp. 815-819.
- ⁷Arena, A. S.; and Nelson, R. C.: The Effect of Asymmetric Vortex Wake Characteristics on a Slender Delta Wing Undergoing Wing Rock Motion, AIAA Paper No. 89-3348, August 1989.
- ⁸Ng, T. T.; Malcolm, G. N.; and Lewis, L. C.: Flow Visualization Study of Delta Wings in Wing-Rock Motion, AIAA Paper No. 89-2187, August 1989.
- ⁹Hsu, C. H.; and Lan, C. E.: Theory of Wing Rock, Journal of Aircraft, Vol. 22, October 1985, pp. 920-924.
- ¹⁰Konstadinopoulos, P.; Mook, D. T.; and Nayfeh, A. H.: Subsonic Wing Rock of Slender Delta Wings, Journal of Aircraft, Vol. 22, March 1985, pp. 223-228.

- ¹¹Elzebda, J. M.; Nayfeh, A. H.; and Mook, D. T.: Development of an Analytical Model of Wing Rock for Slender Delta Wings, Journal of Aircraft, Vol. 26, August 1989, pp. 737-743.
- ¹²Nayfeh, A. H.; Elzebda, J. M.; and Mook, D. T.: Analytical Study of the Subsonic Wing-Rock Phenomenon for Slender Delta Wings, Journal of Aircraft, Vol. 26, September 1989, pp. 805-809.
- ¹³Newsome, R. W.; and Kandil, O. A.: Vortical Flow Aerodynamics - Physical Aspects and Numerical Simulation, AIAA Paper No. 87-0205, January 1987.
- ¹⁴Newsome, R. W.; and Thomas, J. L.: Computation of Leading-Edge Vortex Flows, Proceedings of the Conference on Vortical Flow Aerodynamics, NASA Langley Research Center, Hampton, Virginia, October 8-10, 1985.
- ¹⁵Kandil, O. A.; and Chuang, A.: Influence of Numerical Dissipation in Computing Supersonic Vortex-Dominated Flows, AIAA Paper No. 86-1073, May 1986.
- ¹⁶Chakravarthy, S. R.; and Ota, D. K.: Numerical Issues in Computing Inviscid Supersonic Flow Over Conical Delta Wings, AIAA Paper No. 86-0440, January 1986.
- ¹⁷Murman, E. M.; Powell, K. G.; Miller, D. S.; and Wood, R. M.: Comparisons of Computations and Experimental Data for Leading Edge Vortices - Effects of Yaw and Vortex Flaps, AIAA Paper No. 86-0439, January 1986.
- ¹⁸Murman, E. M.; and Rizzi, A.: Applications of Euler Equations to Sharp Edge Delta Wings With Leading Edge Vortices, AGARD-CP-412, November 1986.
- ¹⁹McMillin, S. N.; Thomas, J. L.; and Murman, E. M.: Euler and Navier-Stokes Solutions for the Leaside Flow Over Delta Wings at Supersonic Speeds, AIAA Paper No. 87-2270, July 1987.
- ²⁰Fujii, K.: A Method to Increase the Accuracy of Vortical Flow Simulations, AIAA Paper No. 88-2562, July 1988.
- ²¹Powell, K. G.; Murman, E. M.; Perez, E. S.; and Baron, J. R.: Total Pressure Loss in Vortical Solutions of the Conical Euler Equations, AIAA Journal, Vol. 25, 1987.

²²Kandil, O. A.; and Chuang, A. H.: Computation of Steady and Unsteady Vortex Dominated Flows, AIAA Paper No. 87-1462, June 1987.

²³Kandil, O. A.; and Chuang, A. H.: Unsteady Navier-Stokes Computations Past Oscillating Delta Wing at High Incidence, AIAA Paper No. 89-0081, January 1989.

²⁴Batina, J. T.: Vortex-Dominated Conical-Flow Computations Using Unstructured Adaptively-Refined Meshes, AIAA Paper No. 89-1816, June 1989.

²⁵Morgan, K.; and Peraire, J.: Finite Element Methods for Compressible Flow, Von Karman Institute for Fluid Dynamics Lecture Series 1987-04, Computational Fluid Dynamics, March 2-6, 1987.

Table 1 Summary of structural parameter values and flow conditions for the free-to-roll calculation.

Parameter	Value
c	0.2820 m
I_{xx}	$0.1776 \times 10^{-3} \text{ Kg m}^2$
μ_x	$0.0 \text{ Kg m}^2/\text{s}$
ρ_∞	0.526 Kg/m^3
a_∞	312 m/s

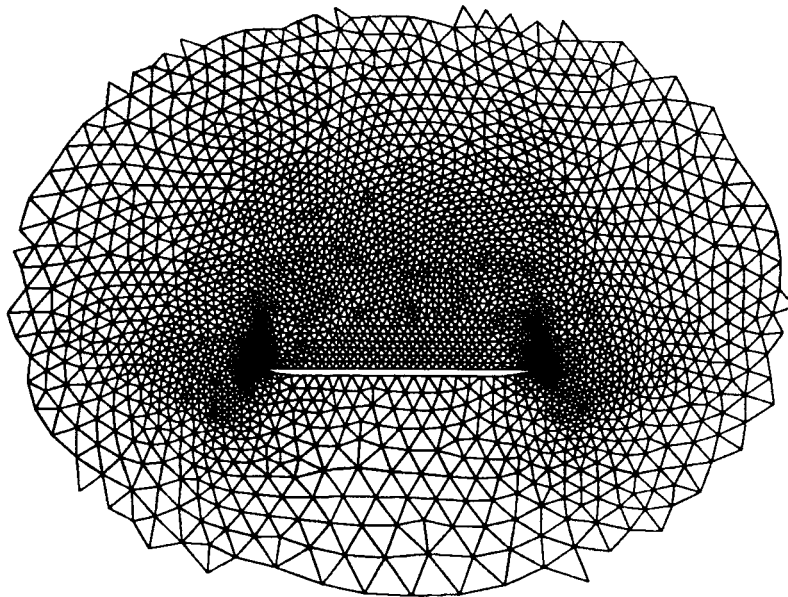


Fig. 1 Partial view of unstructured grid about a 75° swept delta wing.

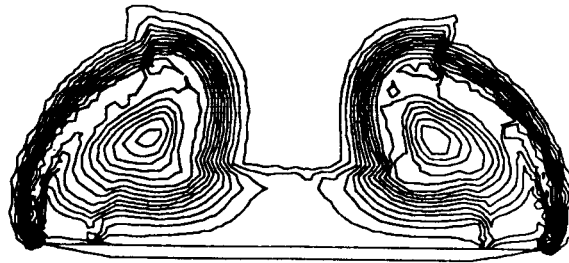


Fig.2 Steady-state total pressure loss contours for a 75° swept delta wing at $M_\infty = 1.2$ and $\alpha = 30^\circ$.

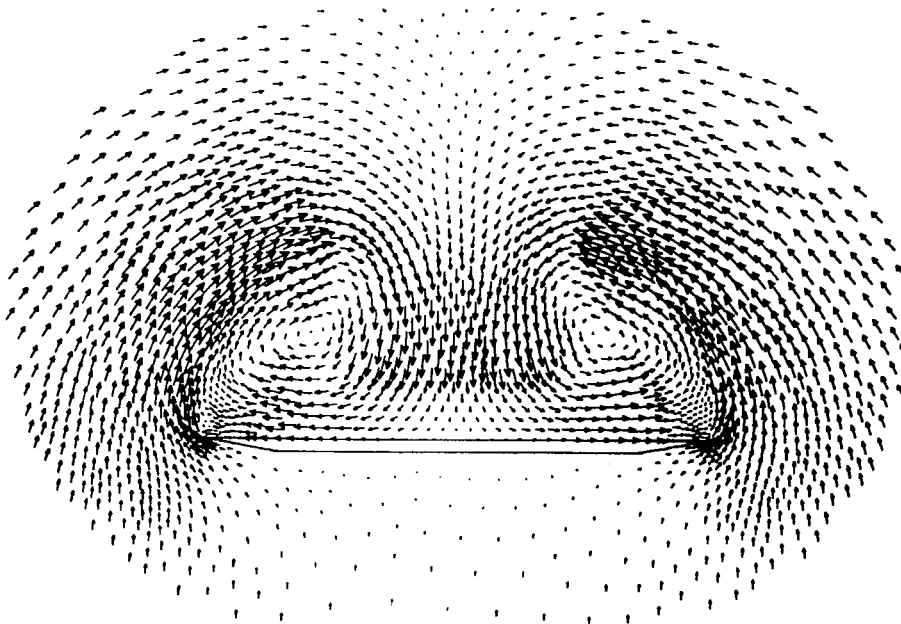


Fig. 3 Steady-state crossflow velocity vectors for a 75° swept delta wing at $M_\infty = 1.2$ and $\alpha = 30^\circ$.

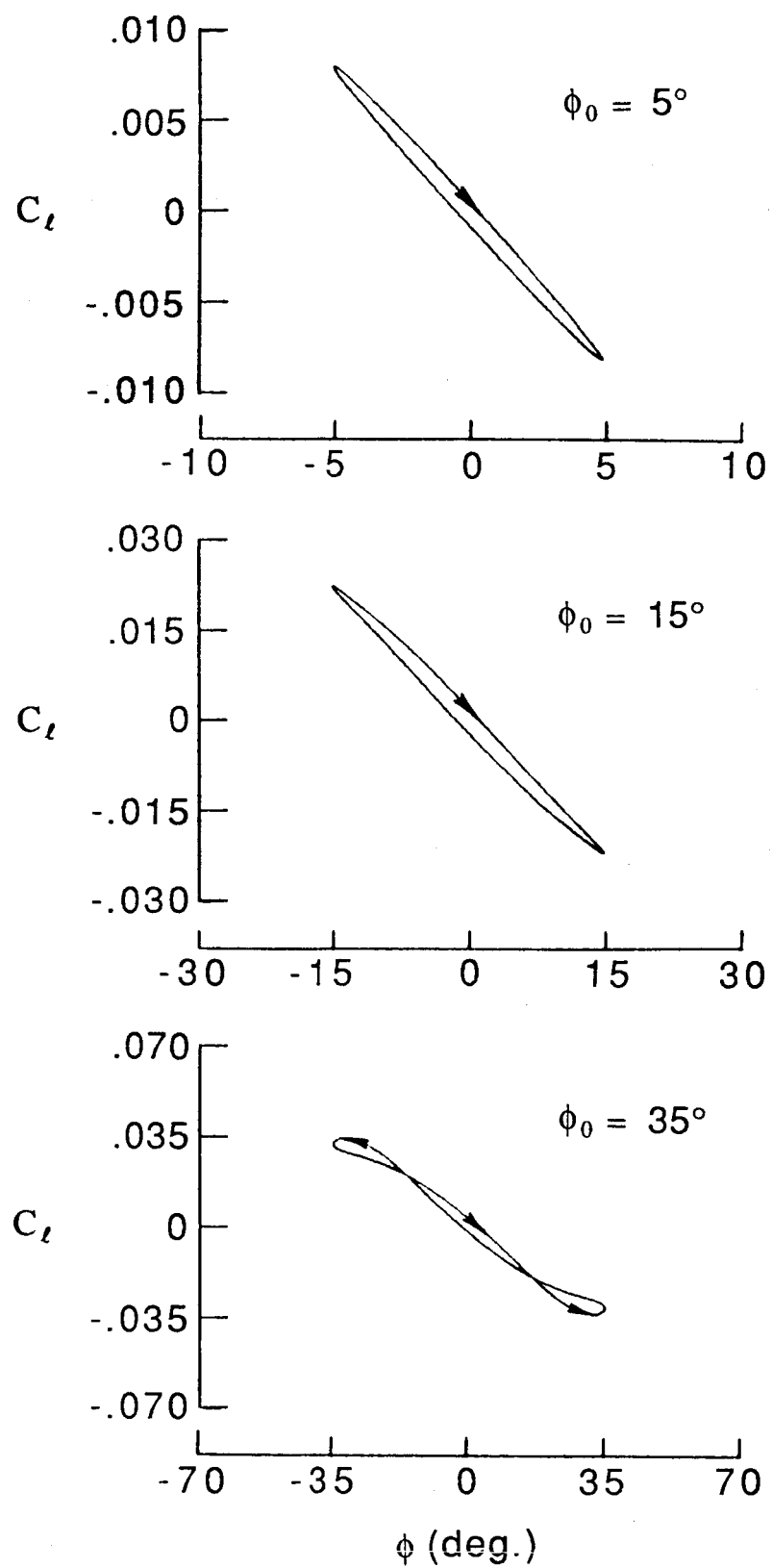


Fig. 4 Rolling moment coefficient versus instantaneous roll angle for a 75° swept delta wing at $M_\infty = 1.2$, $\alpha = 30^\circ$, and $k = 0.3$.

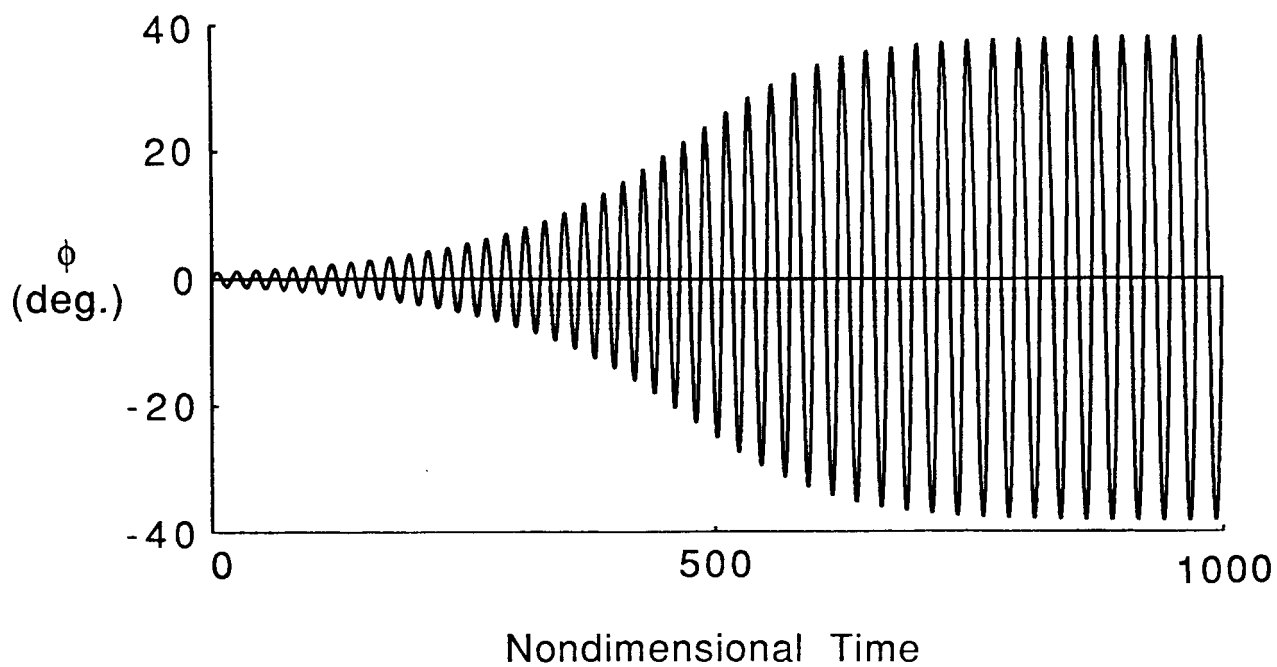


Fig. 5 Free-to-roll time history for a 75° swept delta wing at $M_{\infty} = 1.2$ and $\alpha = 30^\circ$.

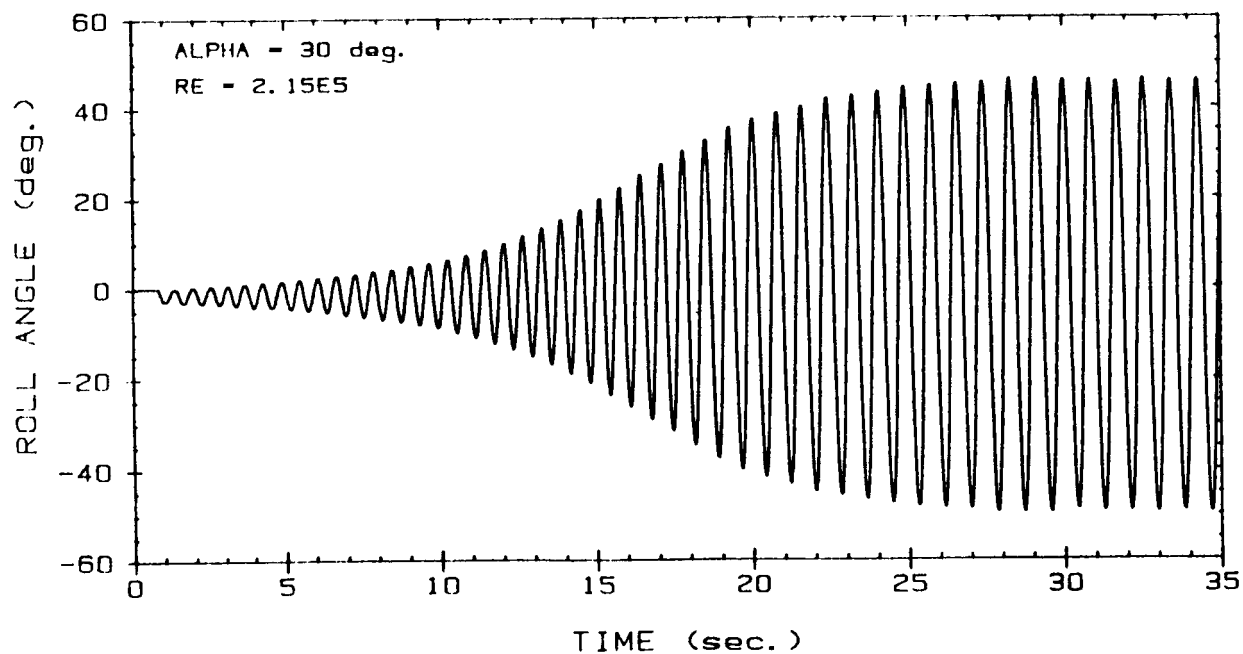


Fig. 6 Wing-rock time history for an 80° swept delta wing at 30° angle of attack (Ref. 7, reprinted with permission from Professor Robert C. Nelson, Notre Dame University).

Report Documentation Page

1. Report No. NASA TM-102609		2. Government Accession No.		3. Recipient's Catalog No.	
4. Title and Subtitle Conical Euler Solution for a Highly-Swept Delta Wing Undergoing Wing-Rock Motion				5. Report Date March 1990	
				6. Performing Organization Code	
7. Author(s) Elizabeth M. Lee and John T. Batina				8. Performing Organization Report No.	
				10. Work Unit No.	
9. Performing Organization Name and Address NASA Langley Research Center Hampton, Virginia 23665-5225				505-63-21-01	
				11. Contract or Grant No.	
12. Sponsoring Agency Name and Address National Aeronautics and Space Administration Washington, D. C. 20546-0001				13. Type of Report and Period Covered Technical Memorandum	
				14. Sponsoring Agency Code	
15. Supplementary Notes					
16. Abstract Modifications to an unsteady conical Euler code for the free-to-roll analysis of highly-swept delta wings are described. The modifications involve the addition of the rolling rigid-body equation of motion for its simultaneous time-integration with the governing flow equations. The flow solver utilized in the Euler code includes a multistage Runge-Kutta time-stepping scheme which uses a finite-volume spatial discretization on an unstructured mesh made up of triangles. Steady and unsteady results are presented for a 75° swept delta wing at a freestream Mach number of 1.2 and angle of attack of 30°. The unsteady results consist of forced harmonic and free-to-roll calculations. The free-to-roll case exhibits a wing rock response produced by unsteady aerodynamics consistent with the aerodynamics of the forced harmonic results. Similarities are shown with a wing-rock time history from a low-speed wind tunnel test.					
17. Key Words (Suggested by Author(s)) Wing Rock Computational Fluid Dynamics Unsteady Aerodynamics Vortical Flow			18. Distribution Statement Unclassified - Unlimited Subject Category - 02		
19. Security Classif. (of this report) Unclassified	20. Security Classif. (of this page) Unclassified		21. No. of pages 17	22. Price A03	